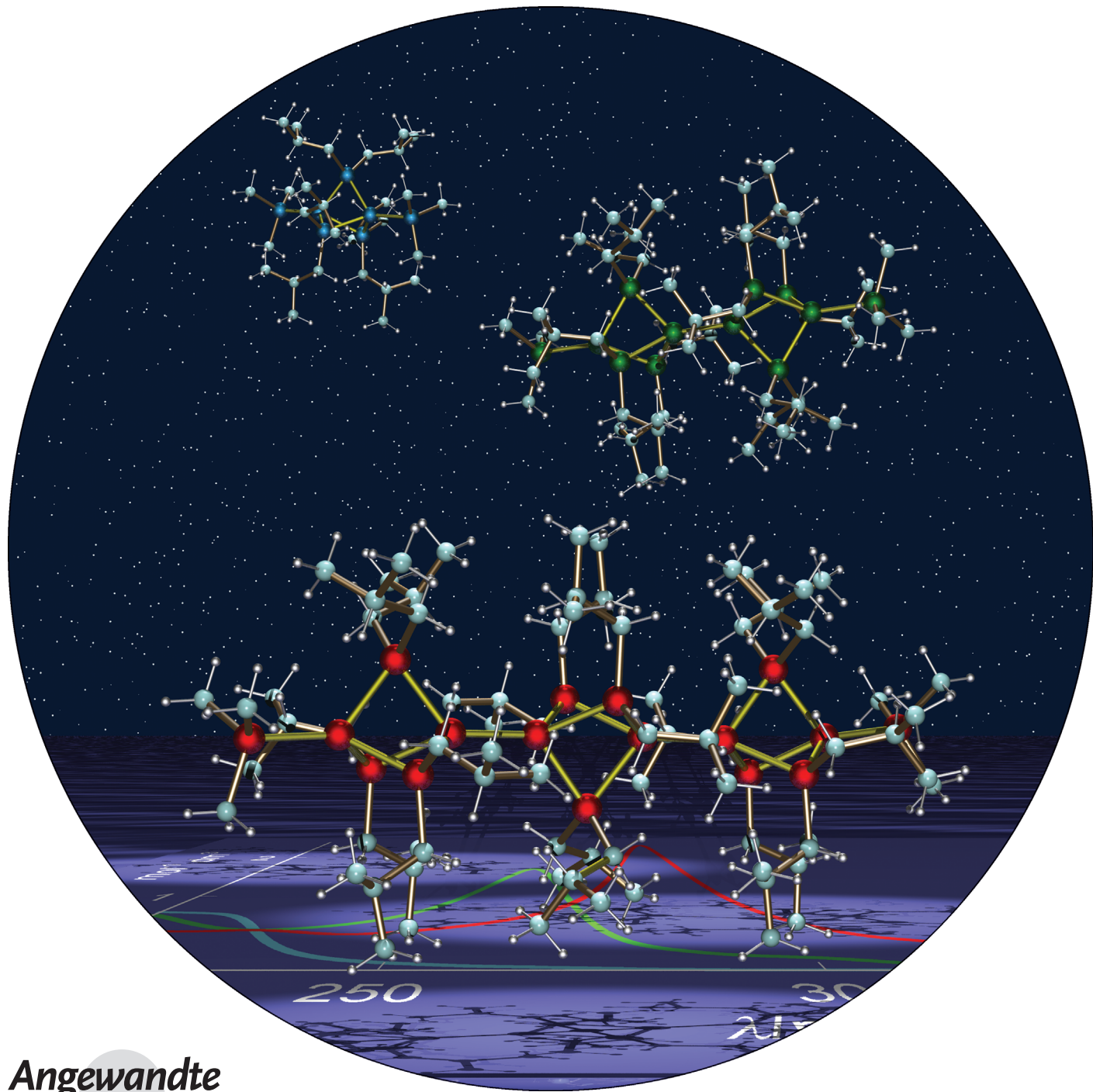


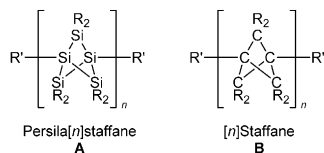
# Persilastaffanes: Design, Synthesis, Structure, and Conjugation between Silicon Cages<sup>\*\*</sup>

Takeaki Iwamoto,\* Daisuke Tsushima, Eunsang Kwon, Shintaro Ishida, and Hiroyuki Isobe

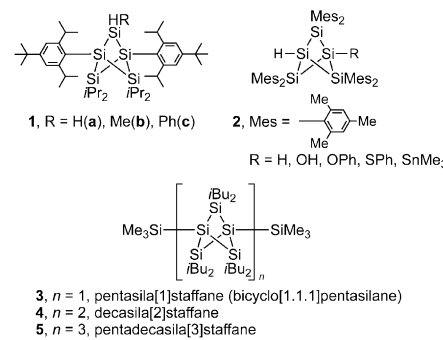


Polycyclic oligosilanes<sup>[1–3]</sup> are interesting silicon compounds because they have  $\sigma$  electrons of Si–Si bonds delocalized over a three-dimensional silicon framework which are often found in crystalline or amorphous silicon and related important silicon clusters.<sup>[4–6]</sup> Although various types of polycyclic oligosilanes have been synthesized and investigated so far, there have been very few studies on catenated polycyclic oligosilanes (oligomers of polycyclic oligosilanes), which should show significant interactions between polycyclic oligosilane cages.<sup>[7–9]</sup>

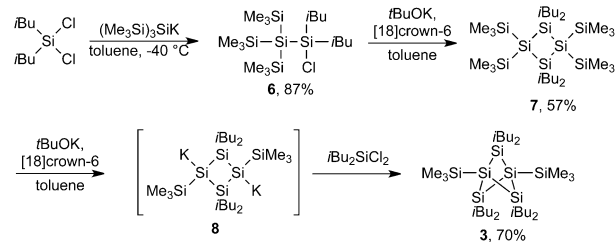
Persila[*n*]staffanes **A** are one of the fascinating unknown catenated polycyclic oligosilanes because they have highly symmetric rodlike structures with bicyclo[1.1.1]pentasilane units catenated at the bridgehead positions and they are predicted by Yamaguchi to have small band gaps because of delocalization of  $\sigma$  electrons along the silicon cages.<sup>[7]</sup> The corresponding all-carbon [*n*]staffanes **B** have been studied extensively by Michl and co-workers.<sup>[10,11]</sup> Although stable bicyclo[1.1.1]pentasilanes bearing aryl substituents **1**<sup>[12]</sup> and **2**<sup>[13]</sup> have been synthesized by the Masamune and Breher,<sup>[14]</sup> no catenated bicyclo[1.1.1]pentasilanes (persila[*n*]staffanes,  $n \geq 2$ ) have been reported. Herein, we would like to report the synthesis and structure of a series of persila[*n*]staffanes **3** ( $n=1$ ), **4** ( $n=2$ ), and **5** ( $n=3$ ) and their remarkable conjugation between bicyclo[1.1.1]pentasilane units.



To synthesize persila[*n*]staffanes, we designed novel bicyclo[1.1.1]pentasilane **3** (persila[1]staffane) as a unit for persila[*n*]staffanes. Compound **3** has 1) alkyl substituents (*i*Bu) on the bridge silicon atoms that cause least electronic perturbation to silicon frameworks and 2) silyl substituents on the bridgehead silicons ( $\text{Me}_3\text{Si}$ ) that can be easily functionalized,<sup>[15]</sup> and hence, **3** should be suitable for investigation of



the intrinsic electronic structure of bicyclo[1.1.1]pentasilane frameworks and extension of bicyclopentasilane units at the bridgehead positions. Compound **3** was synthesized according to the reaction sequence shown in Scheme 1. Reaction of *i*Bu<sub>2</sub>SiCl<sub>2</sub> with 1 equiv of  $(\text{Me}_3\text{Si})_3\text{SiK}$  in toluene gave



**Scheme 1.** Synthesis of persila[1]staffane **3**.

$(\text{Me}_3\text{Si})_3\text{SiSi}(i\text{Bu})_2\text{Cl}$  (**6**) in 87% yield, which was treated with 1 equiv of *t*BuOK to afford 1,1,3,3-tetrasilylcyclotetrasilane **7** in 57% yield.<sup>[16]</sup> Then, treatment of **7** with 2 equiv of *t*BuOK giving bicyclotetrasilane-1,3-diide **8** followed by *i*Bu<sub>2</sub>SiCl<sub>2</sub> afforded **3** as air-stable colorless crystals in 70% yield.<sup>[17,18]</sup> The structure of **3** was determined by NMR spectroscopy, MS spectrometry, and X-ray analysis (Figure 1).

Synthesis of persila[2]staffane **4** and persila[3]staffane **5** are accomplished by stepwise catenation of the bicyclo[1.1.1]pentasilane units through functionalization of their bridgehead silicons of **3** as shown in Schemes 2 and 3. Treatment of bicyclopentasilane **3** with *t*BuOK in the presence of [18]crown-6 (18-c-6) in toluene resulted in the cleavage of bridgehead Si–Si bond to form potassium bicyclo[1.1.1]pentasilanide **9**(18-c-6) in 55% yield. Although a few polycyclic silyl anions have been synthesized,<sup>[19]</sup> compound **9** is the first silyl anion with bicyclo[1.1.1]pentasilane skeleton. When the solution of **9** was treated with an excess amount of 1,2-dibromoethane, 1-bromobicyclo[1.1.1]pentasilane **10** was obtained in 76% yield (from **3**).<sup>[20]</sup> Then, coupling reaction of **9** and **10** provided persila[2]staffane **4** as air-stable colorless crystals in 53% yield. In a similar manner, persila[3]staffane **5** was obtained from **4** in 2% yield in two steps.<sup>[21]</sup> Structures of persilastaffanes **4** and **5** were determined by NMR spectroscopy, MS spectrometry, and X-ray analysis.<sup>[22]</sup>

Molecular structures of persilastaffanes **3–5** determined by X-ray single-crystal analysis are shown in Figure 1.

[\*] Prof. Dr. T. Iwamoto, D. Tsushima, Dr. S. Ishida, Prof. Dr. H. Isobe  
Department of Chemistry, Graduate School of Science  
Tohoku University, Aoba-ku, Sendai 980-8578 (Japan)  
E-mail: iwamoto@m.tohoku.ac.jp

Dr. E. Kwon  
Research and Analytical Center for Giant Molecules  
Graduate School of Science, Tohoku University  
Aoba-ku, Sendai 980-8578 (Japan)

[\*\*] This work was supported by the Ministry of Education, Culture, Sports, Science, and Technology of Japan (Grant-in-Aid for Scientific Research, grant number 20685004, T.I.) and the JST (Research Seeds Quest Program, T.I.). We thank Prof. Dr. Masahiro Hirama and Prof. Dr. Masahiro Terada (Tohoku University) for measurement time of solid-state NMR spectra and Dr. Toshihito Nakai (JEOL RESONANCE) for recording the solid-state <sup>29</sup>Si NMR spectra. D.T. thanks the Global COE program (Molecular Complex Chemistry) for a predoctoral fellowship.

Supporting information for this article is available on the WWW under <http://dx.doi.org/10.1002/anie.201106422>.

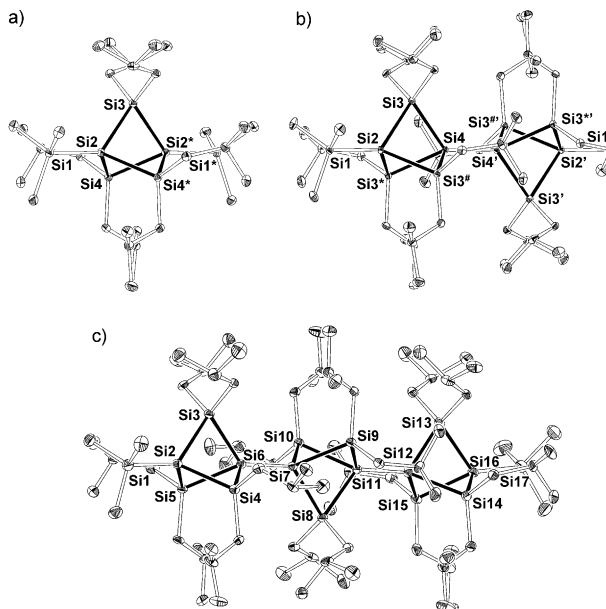
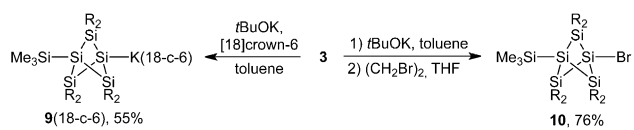
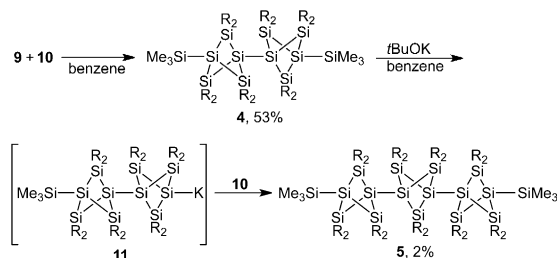


**Figure 1.** ORTEP drawings of a) persila[1]staffane 3, b) persila[2]staffane 4, and c) persila[3]staffane 5. All hydrogen atoms are omitted for clarity. Thermal ellipsoids are shown at the 30% probability level.



**Scheme 2.** Functionalization of 3 (R = *i*Bu).



**Scheme 3.** Synthesis of persila[2]staffane 4 and persila[3]staffane 5 (R = *i*Bu).

Bicyclo[1.1.1]pentasilane **3** (Figure 1a) has a three-fold axis through the bridgehead silicon atoms in the solid state. Similarly to Masamune's bicyclopentasilanes **1** and all-carbon bicyclo[1.1.1]pentanes,<sup>[10]</sup> **3** has a short nonbonded distance between bridgehead silicon atoms (Si2···Si2<sup>\*</sup>) of 2.9768(5) Å, which is much shorter than the sum of van der Waals radii of two silicon atoms (4.20 Å) and close to that of **1a** (2.98 Å),<sup>[12]</sup> and considerably acute intracage Si–Si–Si angles (Si3–Si2–Si4<sup>(\*)</sup> and Si4–Si2–Si4<sup>\*</sup> angles) at the bridgehead silicon atom Si2 (84.6° on average). The exocyclic Si1–Si2 distance of **3** (2.3429(6) Å) is slightly shorter than the endocyclic Si–Si distances of **3** (2.3622(6)–2.3626(6) Å for Si2–Si3 and Si2–Si4), which are lying in the range of those of **1a** (2.32(2)–2.38(1) Å).

Persila[2] and [3]staffanes **4** and **5** adopt almost linear structures. The silicon atoms of the terminal SiMe<sub>3</sub> group and the bridgehead silicon atoms of the bicyclopentasilane cages in **4** lie on the crystallographic three-fold axis, whereas those of **5** deviate slightly from perfect linearity probably because of the crystal packing.<sup>[23]</sup> The neighboring bicyclo[1.1.1]pentasilane cages are almost perfectly staggered with the averaged dihedral angle Si(bridge)–Si(bridgehead)–Si(bridgehead)–Si(bridge) of 180° for **4** and 178.8° for **5**. All the tetrasilane units adopt the all-transoid and all-anti conformation suitable for conjugation between Si–Si bonds in the silicon cages. The endocyclic Si–Si distances of 2.3602(13)–2.3788(13) Å for **4** and 2.355(3)–2.394(3) for **5** are slightly longer than those of **3**. Similarly to **3**, the intercage bridgehead Si–Si distances of **4** (2.360(3) Å for Si4–Si4<sup>\*</sup>) and **5** (2.348(3) and 2.363(3) for Si6–Si7 and Si11–Si12, respectively) as well as the Si(bridgehead)–SiMe<sub>3</sub> distances (2.341(2) Å) are shorter than the endocyclic Si–Si bond. The shorter exocyclic Si–Si bonds observed in **3**–**5** are explained in terms of Bent's rule: an increased s character of the bridgehead silicon orbital in the exocyclic Si–Si bond resulting from the acute intracage Si–Si–Si angles would be responsible for the shorter exocyclic Si–Si bond distance. Interestingly, the long axis of persilastaffanes **3**–**5** are arranged almost parallel in the single crystals (see Figure S15 in the Supporting Information).<sup>[18]</sup> Distances between SiMe<sub>3</sub> silicon atoms at the bridgehead position are 7.6626(7), 12.979(3), and 18.311(6) Å for **3**, **4**, and **5**, respectively. The molecular structures of **3**–**5** show that each addition of bicyclopentasilane units increases the length of the persilastaffane rod by about 5.3 Å, but catenation of the bicyclopentasilane units causes no remarkable change in the structural characteristics of each bicyclopentasilane unit.

The NMR spectra show that compounds **3**–**5** have highly symmetric structures in solution. The <sup>1</sup>H and <sup>13</sup>C NMR spectra of **3**–**5** show a singlet-signal assigned to Me<sub>3</sub>Si groups on the bridgehead silicon atoms and one (for **3** and **4**) or two (for **5**) set(s) of signals due to *i*Bu groups on the bridge silicon atoms suggesting facile rotation around the interbridgehead Si–Si bonds in solution.<sup>[22]</sup>

The most striking spectral feature was found in UV/Vis absorption spectra. As shown in Figure 2, compounds **3**–**5** in hexane show two absorption bands I and II. The intense band I and weak band II of **3** appear at around 220 nm ( $\epsilon =$

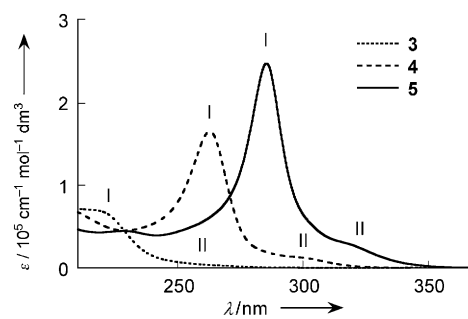
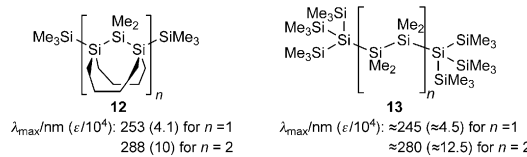


**Figure 2.** UV/Vis absorption spectra of persila[n]staffanes **3** (n = 1, dotted line), **4** (n = 2, broken line), and **5** (n = 3, solid line) in hexane at room temperature.

$6.8 \times 10^4 \text{ cm}^{-1} \text{ mol}^{-1} \text{ dm}^3$ ) and 255 nm (shoulder,  $\epsilon = 5.4 \times 10^3 \text{ cm}^{-1} \text{ mol}^{-1} \text{ dm}^3$ ), respectively.<sup>[24]</sup> Both bands I and II are remarkably red-shifted and increased with increasing the number of bicyclopentasilane cages ( $\lambda_{\text{max}}/\text{nm}$  of bands I and II: 263 and 300 for **4**, 285 and 320 for **5**). Although the red-shift is similar to those observed for  $\sigma \rightarrow \sigma^*$  transitions of **12**<sup>[25]</sup> and **13**<sup>[26]</sup> having all-anti and all-transoid pentasilane and octasilane moieties similar to **3** and **4**, the spectral features of **3** and **4** are different from those of **12** and **13**.



To elucidate the absorption bands of **3**–**5**, we performed DFT calculations for model compounds **3'**–**5'**. The molecular structures of **3**–**5** determined by X-ray analysis were well-reproduced by the structures of **3'**–**5'** optimized at the B3LYP/6-31G(d) level.<sup>[27]</sup> As shown in Figure 3, frontier Kohn–Sham

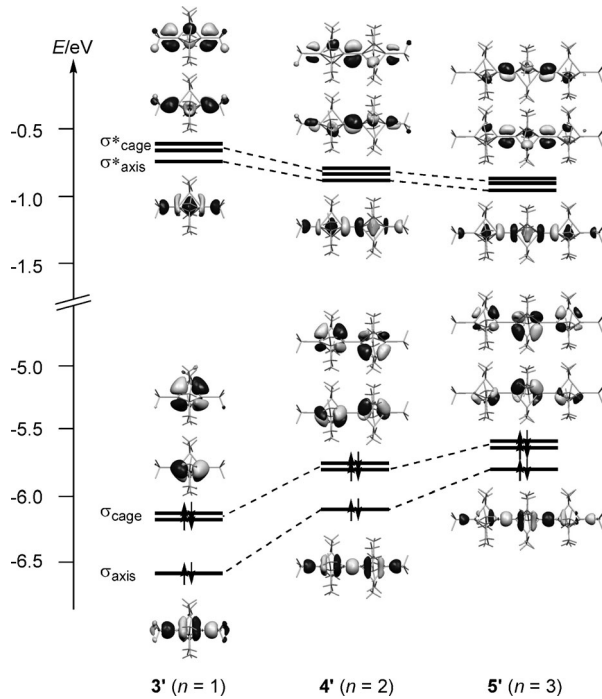
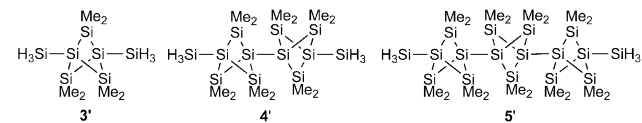


**Figure 3.** Frontier Kohn–Sham orbitals of **3'** ( $n=1$ ), **4'** ( $n=2$ ), and **5'** ( $n=3$ ) calculated at the B3LYP/def2-TZVP//B3LYP/6-31G(d) level.

(KS) orbitals of **3'**–**5'** calculated at the B3LYP/def2-TZVP level are doubly degenerated  $\sigma(\text{Si–Si})$  orbitals in a bicyclo[1.1.1]pentasilane cage with  $\pi$  symmetry relative to the three-fold axis ( $\sigma_{\text{cage}}$ ) and a  $\sigma(\text{Si–Si})$  orbital delocalized mainly over the bridgehead Si–Si bonds with  $\sigma$  symmetry ( $\sigma_{\text{axis}}$ ), and the corresponding  $\sigma_{\text{cage}}^*$  and  $\sigma_{\text{axis}}^*$  orbitals, respectively. With increasing the number of bicyclopentasilane cages, the  $\sigma_{\text{cage}}$

and  $\sigma_{\text{axis}}$  orbitals become higher in energy, while the  $\sigma_{\text{cage}}^*$  and  $\sigma_{\text{axis}}^*$  orbitals become lower in energy. These orbital features would be ascribed to the conjugation between  $\sigma_{\text{cage}}$  orbitals and between the linearly arranged  $\sigma_{\text{axis}}$  orbitals.<sup>[9,28]</sup>

The experimental absorption spectra of **3**–**5** are qualitatively reproduced by the calculated absorption band positions and oscillator strengths of **3'**–**5'**.<sup>[27]</sup> According to the compar-



ison of the experimental and calculated absorption spectra, bands I and II are assignable to the  $\sigma_{\text{axis}} \rightarrow \sigma_{\text{axis}}^*$  transition and the  $\sigma_{\text{cage}} \rightarrow \sigma_{\text{cage}}^*$  transition with a significant contribution of  $\sigma_{\text{cage}} \rightarrow \sigma_{\text{axis}}^*$  transition, respectively.<sup>[29]</sup> The red-shifts of both bands I and II on going from **3** to **5** indicate the remarkable delocalization of  $\sigma$  electrons between the catenated bicyclo[1.1.1]pentasilane cages.<sup>[7]</sup>

In conclusion, we successfully synthesized a series of persila[n]staffanes **3**–**5** ( $n=1$ – $3$ ) through a stepwise catenation and disclosed the considerable delocalization of  $\sigma$  electrons along the catenated silicon cages. Persila[n]staffanes may be fascinating rodlike silicon molecules as linear connectors for novel silicon-based finely defined materials.<sup>[30,31]</sup>

Received: September 10, 2011

Published online: December 7, 2011

**Keywords:** conjugation · oligomerization · silanes · staffanes

- [1] For reviews on oligosilanes and polysilanes, see: a) M. Kumada, K. Tamao, *Adv. Organomet. Chem.* **1968**, *6*, 19–117; b) R. West, *J. Organomet. Chem.* **1986**, *300*, 327–346; c) R. D. Miller, J. Michl, *Chem. Rev.* **1989**, *89*, 1359–1410; d) H. A. Fogarty, D. L. Casher, R. Imhof, T. Schepers, D. W. Rooklin, J. Michl, *Pure Appl. Chem.* **2003**, *75*, 999–1020.
- [2] For reviews of cyclic polysilanes and silicon cage compounds, see: a) E. Hengge, R. Janoschek, *Chem. Rev.* **1995**, *95*, 1495–1526; b) A. Sekiguchi, H. Sakurai, *Adv. Organomet. Chem.* **1995**, *37*, 1–38; c) A. Sekiguchi, S. Nagase in *The Chemistry of Organic Silicon Compounds*, Vol. 2 (Eds.: Z. Rappoport, Y. Apeloig), Wiley, New York, **1998**, chap. 5, pp. 119–152.
- [3] For reviews of ladder polysilanes, see: a) S. Kyushin, H. Matsumoto, *Adv. Organomet. Chem.* **2003**, *49*, 133–166; b) H. Matsumoto, S. Kyushin, M. Unno, R. Tanaka, *J. Organomet. Chem.* **2006**, *691*, 52–63.
- [4] For a bicyclic oligosilane with a Si=Si double bond as a model for Si(001) surface, see: a) H. Kobayashi, T. Iwamoto, M. Kira, *J. Am. Chem. Soc.* **2005**, *127*, 15376–15377. For a silaadamantane having a partial structure of single-crystalline silicon, see: b) J. Fischer, J. Baumgartner, C. Marschner, *Science* **2005**, *310*, 825. For tricyclic hexasilanes as isomers of hexasilabenzene, see: c) K. Abersfelder, A. J. P. White, H. S. Rzepa, D. Scheschke, *Science* **2010**, *327*, 564–566; d) K. Abersfelder, A. J. P. White, R. J. F. Berger, H. S. Rzepa, D. Scheschke, *Angew. Chem.* **2011**, *123*, 8082–8086; *Angew. Chem. Int. Ed.* **2011**, *50*, 7936–

7939. For a tricyclohexasilane as an isomer of hexasila-1,4-diene, see: e) T. Iwamoto, K. Uchiyama, C. Kabuto, M. Kira, *Chem. Lett.* **2007**, 36, 368–369.

[5] a) N. Sandström, H. Ottoson, *Chem. Eur. J.* **2005**, 11, 5067–5079; b) Y. Fujimoto, T. Koretsune, S. Saito, T. Miyake, A. Oshiyama, *New J. Phys.* **2008**, 10, 083001.

[6] For a review of silicon clathrate, see: S. Yamanaka, *Dalton Trans.* **2010**, 39, 1901–1915.

[7] Y. Yamaguchi, *Synth. Met.* **1994**, 62, 23–26.

[8] For dimethylsilylene-bridged bis(bicyclo[2.2.2]octasilanes) and bis(bicyclo[2.2.1]heptasilanes), see: a) A. Wallner, J. Hlina, T. Konopa, H. Wagner, J. Baumgartner, C. Marschner, *Organometallics* **2010**, 29, 2660–2675. For cyclohexasilanyl-substituted bicyclo[2.2.2]octasilane, see: b) R. Fischer, T. Konopa, S. Ully, J. Baumgartner, C. Marschner, *J. Organomet. Chem.* **2003**, 685, 79–92. See also Refs. [2a] and [4b].

[9] The electronic delocalization along the one-dimensionally arranged Si–Si bonds in disilatriptycene oligomers was reported by Tamao, Tsuji, and co-workers. S. Sase, Y.-S. Cho, A. Kawachi, A. Wakamiya, S. Yamaguchi, H. Tsuji, K. Tamao, *Organometallics* **2008**, 27, 5441–5445.

[10] For reviews of *[n]*staffanes, see: a) P. Kaszynski, J. Michl, *Adv. Strain Org. Chem.* **1995**, 4, 283–331; b) M. D. Levin, P. Kaszynski, J. Michl, *Chem. Rev.* **2000**, 100, 169–234.

[11] a) P. Kaszynski, J. Michl, *J. Am. Chem. Soc.* **1988**, 110, 5225–5526; b) P. Kaszynski, A. C. Friedli, J. Michl, *J. Am. Chem. Soc.* **1992**, 114, 601–620.

[12] Y. Kabe, T. Kawase, J. Okada, O. Yamashita, M. Goto, S. Masamune, *Angew. Chem.* **1990**, 102, 823–825; *Angew. Chem. Int. Ed. Engl.* **1990**, 29, 794–796.

[13] D. Nied, R. Köppe, W. Klopper, H. Schnöckel, F. Breher, *J. Am. Chem. Soc.* **2010**, 132, 10264–10265.

[14] Orudzhaeva and Suleimanov have proposed the generation of octamethylbicyclo[1.1.1]pentasilane by using mass spectrometry; K. N. Orudzhaeva, G. Z. Suleimanov, *Azerb. Khim. Zh.* **2004**, 1, 87.

[15] C. Marschner, *Eur. J. Inorg. Chem.* **1998**, 221–226.

[16]  $(\text{Me}_3\text{Si})_2\text{SiKSi}(\text{iBu})_2\text{Cl}$  may be an intermediate for formation of **8**. Marschner and co-workers reported that thermolysis of  $(\text{Me}_3\text{Si})_2\text{SiKSi}(\text{SiMe}_3)_2\text{F}$  gave octakis(trimethylsilyl)cyclotetrasilane. R. Fischer, J. Baumgartner, G. Kickelbick, C. Marschner, *J. Am. Chem. Soc.* **2003**, 125, 3414–3415.

[17] Similarly, Masamune's bicyclo[1.1.1]pentasilanes **1** were synthesized by the reaction of cycloctetrasilane-1,3-diide with dihalosilanes. See Ref. [12]. For examples of preparation of cycloctetrasilane-1,3-diide, see: a) S. Kyushin, H. Kawai, H. Matsumoto, *Organometallics* **2004**, 23, 311–313; b) R. Fischer, T. Konopa, J. Baumgartner, C. Marschner, *Organometallics* **2004**, 23, 1899–1907.

[18] CCDC 842825 (**3**), 842826 (**4**), 842827 (**5**), and 842828 (**7**) contain the supplementary crystallographic data for this paper. These data can be obtained free of charge from The Cambridge Crystallographic Data Centre via [www.ccdc.cam.ac.uk/data\\_request/cif](http://www.ccdc.cam.ac.uk/data_request/cif).

[19] For examples of silicon cage anions, see: a) M. Ichinohe, M. Toyoshima, R. Kinjo, A. Sekiguchi, *J. Am. Chem. Soc.* **2003**, 125, 13328–13329; b) W. Setaka, N. Hamada, M. Kira, *Chem. Lett.* **2004**, 33, 626–627; c) V. Y. Lee, T. Yokoyama, K. Takanashi, A. Sekiguchi, *Chem. Eur. J.* **2009**, 15, 8401–8404; d) T. M. Klapötke, S. K. Vasisht, G. Fischer, P. Meyer, *J. Organomet. Chem.* **2010**, 695, 667–672. See also, Ref. [8a].

[20] Treatment of **9** with 1 equiv of 1,2-dibromoethane gave a complex mixture with a trace amount of oxidative coupling product, persila[2]staffane **4**.

[21] Although **5** forms in a moderate yield (about 25%), repeated purification of **5** using preparative gel permeation chromatography because of the poor solubility of **5** resulted in a low yield.

[22] The  $^{29}\text{Si}$  resonance ( $\delta\text{Si}$ ) due to bridgehead silicon nuclei of **3** appeared at  $-99.7$  ppm in  $[\text{D}_6]\text{benzene}$ , which are close to those of Masamune's bicyclo[1.1.1]pentane **1** ( $\delta\text{Si} = -96.5, -91.9$ , and  $-89.9$  ppm for **1a**, **1b**, and **1c**, respectively).<sup>[12]</sup> Because measurement of  $\delta\text{Si}$  of **4** and **5** failed due to their poor solubility, solid-state  $^{29}\text{Si}$  NMR (CP/MAS) spectra of **3–5** were recorded. The  $\delta\text{Si}$  assignable to bridgehead silicon nuclei appeared at  $-101.6$  ppm for **3**,  $-107.0$  and  $-109.5$  ppm for **4**,  $-108.3$  (overlapped) and  $-115.1$  for **5**. For details, see the Supporting Information.

[23] Similar deviation from the perfect linearity have been observed in *[n]*staffanes. A. C. Friedli, V. M. Lynch, P. Kaszynski, J. Michl, *Acta Crystallogr. B* **1990**, 46, 377–389.

[24] Marschner and co-workers reported that 1,4-bis(trimethylsilyl)bicyclo[2.2.2]octasilane shows two absorption bands at  $210\text{ nm}$  ( $\epsilon = 6.1 \times 10^4\text{ cm}^{-1}\text{ mol}^{-1}\text{ dm}^3$ ) and around  $240\text{ nm}$  ( $\epsilon \approx 2 \times 10^4\text{ cm}^{-1}\text{ mol}^{-1}\text{ dm}^3$ ). A. Wallner, M. Hölbling, J. Baumgartner, C. Marschner, *Silicon Chem.* **2007**, 3, 175–185.

[25] a) H. Tsuji, A. Fukazawa, S. Yamaguchi, A. Toshimitsu, K. Tamao, *Organometallics* **2004**, 23, 3375–3377; b) A. Fukazawa, H. Tsuji, K. Tamao, *J. Am. Chem. Soc.* **2006**, 128, 6800–6801.

[26] C. Marschner, J. Baumgartner, A. Wallner, *Dalton Trans.* **2006**, 5667–5674.

[27] For details of the theoretical study see the Supporting Information.

[28] Remarkable interactions between linearly arranged bridgehead C–C bond orbitals in *[n]*staffyl radicals were observed. A. J. McKinley, P. B. Ibrahim, V. Balaji, J. Michl, *J. Am. Chem. Soc.* **1992**, 114, 10631–10637.

[29] The small activation energy for rotation around the interbridgehead Si–Si bond in persila[2]staffane **4'** of  $2.6\text{ kJ mol}^{-1}$  calculated at the B3LYP/6-31G(d) level supports a facile rotation around the Si–Si bond(s) in **4** and **5** in solution. TD-DFT calculations suggests that the facile rotation would not affect remarkably the spectral feature of the absorption spectra of persilastaffanes because the  $\sigma_{\text{axis}} \rightarrow \sigma_{\text{axis}}^*$  and  $\sigma_{\text{cage}} \rightarrow \sigma_{\text{cage}}^*$  transitions for **4'** in the eclipsed form calculated at the B3LYP/def2-TZVP level at 246 and 297 nm, respectively, are similar to those of **4'** in the optimized staggered form (251 and 298 nm).

[30] P. F. H. Schwab, M. D. Levin, J. Michl, *Chem. Rev.* **1999**, 99, 1863–1934.

[31] Examples of bicyclo[1.1.1]pentanes as rigid linear carbon connectors, see: a) R. Gleiter, K.-H. Pfeifer, G. Szeimeis, U. Benz, *Angew. Chem.* **1990**, 102, 418–420; *Angew. Chem. Int. Ed. Engl.* **1990**, 29, 413–415; b) S. Mazières, M. K. Raymond, G. Raabe, A. Prodi, J. Michl, *J. Am. Chem. Soc.* **1997**, 119, 6682–6683; c) A. de Meijere, L. Zhao, V. N. Belov, M. Bossi, M. Noltemeyer, S. W. Hell, *Chem. Eur. J.* **2007**, 13, 2503–2516.